GLP-1-mediated delivery of the PPARα/γ dual-agonist Tesaglitazar improves obesity and glucose metabolism in mice

Carmelo Quarta
University of Bordeaux https://orcid.org/0000-0002-1352-4239
Kerstin Stemmer
Helmholtz Zentrum München
Aaron Novikoff
Helmholtz Zentrum München https://orcid.org/0000-0002-4838-001X
Bin Yang
Novo Nordisk (United States) https://orcid.org/0000-0003-1180-6184
Felix Klingelhuber
Helmholtz Zentrum München
Alexandra Harger
Helmholtz Zentrum München
Mostafa Bakhti
Institute of Diabetes and Regeneration Research, Helmholtz Center Munich, https://orcid.org/0000-0002-2307-1122
Aimée Bastidas-Ponce
Helmholtz Zentrum München
Eric Bauge
Inserm
Christoffer Clemmensen
University of Copenhagen https://orcid.org/0000-0003-2456-9667
Gustav Colldén
Institute for Diabetes and Obesity, Helmholtz Diabetes Center, Helmholtz Zentrum München, 85764, Neuherberg, Germany
Perla Cota
Helmholtz Zentrum München
Daniel Drucker
Mt. Sinai Hospital https://orcid.org/0000-0001-6688-8127
Cristina García-Cáceres
Institute for Diabetes and Obesity, Helmholtz Diabetes Center, Helmholtz Zentrum München, German Research Center for Environmental Health (GmbH), Neuherberg, Germany. https://orcid.org/0000-0001-

6376-9448
Gerald Grandl
Helmholtz Zentrum München
Nathalie Hennuyer
Institut Pasteur de Lille
Stephan Herzig
Helmholtz Zentrum Munich https://orcid.org/0000-0003-3950-3652
Susanna Hofmann
Helmholtz Zentrum München https://orcid.org/0000-0001-7682-5840
Konxhe Kulaj
Helmholtz Zentrum München
Fanny Lalloyer
Inserm
Heiko Lickert
Helmholtz Zentrum München https://orcid.org/0000-0002-4597-8825
Gandhari Maity
Helmholtz Zentrum München
Diego Perez-Tilve
University of Cincinnati https://orcid.org/0000-0002-0351-4133
Miguel A. Sanchez-Garrido
University of Cordoba
Qian Zhang
Helmholtz Zentrum München
Bard Staels
Pasteur Lille https://orcid.org/0000-0002-3784-1503
Natalie Krahmer
Helmholtz Diabetes Center
Richard DiMarchi
Indiana University Bloomington https://orcid.org/0000-0003-0220-4085
Matthias Tschoep
Helmholtz Zentrum Muenchen and Technical University of Munich https://orcid.org/0000-0002-4744-371X
Brian Finan
Novo Nordisk Research Center Indianapolis https://orcid.org/0000-0002-6467-0447
Timo Müller (**timo.mueller@helmholtz-muenchen.de**)
Helmholtz Zentrum München https://orcid.org/0000-0002-0624-9339

Article

Keywords: PPARα/γ, hyperglycemia, insulin resistance

Posted Date: November 30th, 2021

DOI: https://doi.org/10.21203/rs.3.rs-1081959/v1

Version of Record: A version of this preprint was published at Nature Metabolism on August 22nd, 2022.
See the published version at https://doi.org/10.1038/s42255-022-00617-6.

Abstract

Dual-agonists activating the peroxisome proliferator-activated receptors alpha and gamma (PPARα/γ) have shown beneficial effects on glucose and lipid metabolism in patients with type 2 diabetes, but their development was discontinued due to unfavorable cardiovascular and/or renal effects. Here we report the design and preclinical evaluation of a molecule that covalently links the PPARα/γ dual-agonist Tesaglitazar to GLP-1 to allow for the GLP-1 receptor-dependent delivery of Tesaglitazar. GLP-1/Tesaglitazar does not differ from matched GLP-1 in GLP-1R signaling, but shows GLP-1R-dependent PPARγ-RXR heterodimerization with enhanced efficacy to improve body weight, food intake, and glucose metabolism relative to GLP-1 or Tesaglitazar in mice with diet- and genetically-induced obesity. The conjugate fails to affect body weight and glucose metabolism in GLP-1R knockout (ko) mice and shows preserved effects in DIO mice at doses subthreshold for GLP-1 and Tesaglitazar to improve metabolism. Consistent with the GLP-1R expression pattern, LC/MS-based proteomics identified a series of novel PPAR protein targets in the hypothalamus that are acutely upregulated by Tesaglitazar and by GLP-1/Tesaglitazar, but not by treatment with GLP-1. Collectively, our data show that GLP-1/Tesaglitazar improves energy and glucose metabolism with superior efficacy to GLP-1 or Tesaglitazar alone and suggest that this conjugate holds therapeutic value to treat hyperglycemia and insulin resistance.

Introduction

The peroxisome proliferator-activated receptors alpha and gamma (PPARα/γ) play important roles in the regulation of energy, lipid and glucose metabolism[1]. PPARs are nuclear transcription factors which upon ligand activation heterodimerize with the 9-cis retinoic acid receptor (RXR) to promote target gene expression via binding to DNA response elements[2]. While selective activation of PPARα by fibric acid derivates (fibrates) primarily improves hepatic lipid and cholesterol metabolism[3], the selective activation of PPARγ by thiazolidinediones (TZDs) enhances insulin sensitivity in peripheral tissues such as the adipose tissue, liver and skeletal muscle[4]. Although predominantly expressed in the adipose tissue[4], PPARγ mRNA and immunoreactivity has also been detected in hypothalamic nuclei governing energy balance[5], and third ventricle adenoviral-mediated overexpression of PPARγ decreases food intake in lean and diet-induced obese (DIO) mice[6]. Inhibition of food intake by hypothalamic PPARγ activation is, however, not undisputed since also viral-mediated overexpression of PPARγ in the hypothalamus, or administration of the PPARγ agonist Rosiglitazar into the third ventricle, has been shown to increase food intake and body weight in rats[7]. Also systemic activation of PPARγ increases food intake and body weight in rodents[8] and neuron-specific deletion of PPARγ decreases body weight and food intake in mice fed a high-fat diet (HFD)[9]. Fibrates and TZDs have both shown beneficial cardiovascular effects in clinical trials[3,10,11], which together with their complementary action on glucose and lipid metabolism spurred the development of PPARα/γ dual-agonists (Glitazars) for the treatment of type 2 diabetes (T2D) and dyslipidemia[1]. These agents effectively improved glucose and lipid metabolism in clinical trials[12,13], however, the development of many Glitazars was terminated due to unfavorable effects on the

cardiovascular and/or renal system[14]. Adverse effects of Glitazars may include signs of myopathy and muscle catabolism, fluid retention, renal damage, weight gain, peripheral edema and early indications of an increased cardiovascular risk[15].

Tesaglitazar is a PPARα/γ dual-agonist, which in phase II and III clinical trials improved glucose and lipid metabolism with greater efficacy relative to selective PPARγ agonism[13,16–20]. Unfavorable effects of Tesaglitazar are dose-dependent and may include undesired weight gain, increased serum levels of creatinine, and decreased glomerular filtration[13,16,18,19]. In 2006, the development of Tesaglitazar was terminated based on an estimated benefit/risk profile that was not expected to be superior to existing therapies.

Here we report the preclinical pharmacological evaluation of a single molecule conjugate of Tesaglitazar covalently attached to the incretin hormone glucagon-like peptide-1 (GLP-1). We hypothesized that the insulinotropic effect of GLP-1 would synergize with the insulin-sensitizing effect of Tesaglitazar to optimize glucose handling, while the body weight lowering effect of GLP-1 would buffer against the obesogenic nature of PPARγ agonism. We further hypothesized that GLP-1-mediated delivery of Tesaglitazar would provide beneficial glucometabolic effects at doses subthreshold for each monotherapy, thereby improving systemic metabolism at more tolerable doses. In HEK293 cells, we show that GLP-1/Tesaglitazar does not differ from the matched GLP-1 backbone in terms of ligand-induced GLP-1 receptor (GLP-1R) activation, internalization or degradation. GLP-1/Tesaglitazar shows GLP-1R-dependent PPARγ-RXR heterodimerization and enhanced *in vivo* efficacy to reduce body weight and food intake, and to improve glucose metabolism relative to treatment with GLP-1 or Tesaglitazar alone in mice with diet- and genetically-induced obesity. The ability of GLP-1/Tesaglitazar to decrease body weight and to improve glucose control is absent in GLP-1R knockout (ko) mice and is preserved in DIO mice even at doses subthreshold for GLP-1 and Tesaglitazar alone to improve metabolism. In line with previous reports indicating that PPARγ may act on hypothalamic neurocircuitries[5,6], we identified a series of novel PPAR protein targets in the hypothalamus that are acutely upregulated by Tesaglitazar and by GLP-1/Tesaglitazar, but not by treatment with GLP-1. Collectively, our data identify a series of novel Tesaglitazar targets in the hypothalamus and show that GLP-1/Tesaglitazar improves body weight, food intake, and glucose metabolism with superior efficacy relative to treatment with GLP-1 or Tesaglitazar alone. Our data suggest that GLP-1/Tesaglitazar might hold therapeutic value to treat conditions characterized by hyperglycemia and insulin resistance.

Material And Methods

Compound synthesis

Peptidyl-resin with modified GLP - 1 backbone sequence of Boc-His(Trt) – aib - Glu(OtBu) – Gly – Thr(tBu) – Phe – Thr(tBu) – Ser(tBu) – Asp(OtBu) – Val – Ser(tBu) – Ser(tBu) – Tyr(tBu) – Leu – Glu(OtBu) – Glu(OtBu) – Gln(Trt) – Ala – Ala – Lys(Boc) – Glu(OtBu) – Phe – Ile – Ala – Trp – Leu – Val – Lys(Boc) – Gly – Gly – Pro – Ser(tBu) – Ser(tBu) – Gly – Ala – Pro – Pro – Pro – Ser(tBu) - Lys(Mtt) –

amide resin was assembled by automated Fmoc/tBu solid-phase chemistry starting with 0.1mmole of H-Rink Amide ChemMatrix® (PCAS BioMatrix Inc, Saint-Jean-sur-Richelieu, Quebec, Canada) on a Symphony Peptide Synthesizer (Peptide Technology, Tucson, AZ). All Fmoc-amino acids were coupled with 6-Cl-HOBt / DIC activation in DMF. The Fmoc were removed by 20% piperidine in DMF. After the Mtt removal by treating the peptidyl-resin with 1 - 2% TFA / 5% Tis in DCM, Fmoc – Glu - OtBu was coupled with 6-Cl-HOBt / DIC in DMF. Fmoc was deprotected and Tesaglitazar / (S) – 2 – Ethoxy – 3 - (4 - (4 - ((methylsulfonyl)oxy) phenethoxy) phenyl) propanoic acid (Astatech Inc, Bristol, PA) was coupled with 6-Cl-HOBt / DIC in DMF with 3 - fold excess. GLP - 1 – Tesaglitazar conjugate peptide was cleaved from the resin with 10 ml TFA cleavage cocktail containing 8.5 ml TFA, 0.5 ml water, 0.5 ml Tis (triisopropylsilane), 0.25 g phenol and 0.25 ml 2 - mercaptoethanol for 2h. Peptide was precipitated with cold ether, dissolved in 20% acetonitrile (ACN) containing 2% acetic acid and injected to a Luna 19 x 250nm / 10 µm C8 column (Phenomenex, Torrance, CA) to purify with 0.1%TFA / ACN eluent solvents in a Waters 2545 preparative HPLC instrument. Peptide molecular weight characterization was measured by liquid chromatography–mass spectrometry on an Agilent 1260 Infinity/6120 Quadrupole instrument with a Kinetex C8 column with an eluent gradient of 10% – 80% 0.05% ACN. The purified GLP – 1 - Tesaglitazar peptide (HPLC > 95%) was characterized with molecular mass of 1178.5 / [M + 4H]4+ and 1570.8 / [M + 3H]3+ , which consistent with the theoretically calculated molecular weight 4710.1 with formula $C_{214}H_{315}N_{49}O_{69}S$.

Animals

C57BL/6J mice and Lepr^{db} (db/db) mice were purchased from the Jackson Laboratory. *Glp1r*$^{-/-}$ mice were kindly provided by Daniel Drucker (University of Toronto, CA). All wt and ko mice used in our studies were bred on a C57BL/6J background. Mice were double-housed and kept in a constant environment with the ambient temperature set to 22 ± 2°C with constant humidity (45 – 65%) and a 12h/12h light/dark cycle. For studies in DIO mice, male C57BL/6J mice were fed with a high-fat diet (HFD) comprising 58% kcal from fat (D12331; Research Diets, New Brunswick, NJ). db/db mice were fed with a regular chow diet throughout the study. At the beginning of each experiment, mice were equally distributed into experimental groups according to their body weight and body composition. All animal studies were approved by the State of Bavaria, Germany, or the IACUC of the University of Cincinnati, OH, USA. Compounds were dissolved in PBS and were subcutaneously administered with a volume of 5 μl/g body weight in the indicated doses.

Body composition analysis:

Fat and lean tissue mass were measured via Nuclear Magnetic Resonance (NMR) technology (EchoMRI, Houston, TX, USA).

Glucose- and insulin tolerance tests (GTT/ITT):

Glucose tolerance was assessed in 6 h fasted mice after intraperitoneal (i.p) injection of 1.75 g glucose per kg body weight (DIO mice). Insulin tolerance was assessed in 6 h fasted mice after i.p. injection of either 0.75 U Insulin per gram body weight (DIO mice) or 1 U Insulin per gram body weight (db/db mice) (Humalog, Eli Lilly, Indianapolis, IN, USA). Tail vein blood glucose was subsequently measured using a handheld glucometer (TheraSense Freestyle) at baseline and after 15, 30, 60 and 120 min.

Plasma creatinine

Plasma creatinine was measured by a fluorometric creatinine assay kit (Cat#: ab65340, Abcam, Cambridge, United Kingdom) based on the manufacturer's instruction.

Glucose-stimulated insulin secretion (GSIS) in primary murine islets

Isolation of islets was performed by collagenase P digestion of the wt adult pancreas. 3 mL of collagenase P (1 mg/mL) was injected into the bile duct, and the perfused pancreas was consequently dissected and placed into 3 mL collagenase P for 15 min at 37 °C. Then, 10 mL of G-solution (HBSS + 1% BSA) was added, followed by 2 min centrifugation at 1600 rpm at 4 °C. Pellets were re-suspended in 5.5 mL of gradient preparation (5 mL 10% RPMI + 3 mL 40% Optiprep/ per sample) and placed on top of 2.5 mL of the same solution. To form a 3-layers gradient, 6 mL of G-solution was added on the top. Samples were then subjected to 10 min centrifugation at 1700 rpm. Finally, the interphase between the upper and the middle layers of the gradient was harvested and filtered through a 70 µm Nylon filter. The eluent was washed with G-solution, and the islets were handpicked under the microscope. For GSIS analysis, the isolated islets were cultured overnight before being transferred to a 96-well plate containing modified Krebs Ringer phosphate Hepes (KRPH) buffer with 1 mM glucose for 1 h. Afterwards, islets were exposed to equal concentrations of the compounds (3 nM) at the same time when undergoing glucose concentrations of 16.8 mM (2 h each). Insulin was quantified from the supernatant. Finally, the islets were lysed for DNA extraction. Insulin concentrations were measured using an ultrasensitive insulin ELISA kit (Cristal Chem). The analysis was performed using a standard curve and the data were normalized to total content of DNA.

Cell culture and transfection

HEK293T cells were cultured in Dulbecco's Modified Eagle Medium (DMEM, Cat #: 11995073, Life Technologies, Carlsbad, CA, USA) supplemented with 10% heat-inactivated fetal bovine serum (FBS, Cat

#: 10500064, Life Technologies, Carlsbad, CA, USA), 100 IU/mL of penicillin, and 100 µg/mL of streptomycin solution (Pen-Strep, Cat #: P4333, Sigma–Aldrich, St. Louis, MO, USA). HEK293T cells (700,000/well) were seeded in 6-well plates and incubated to 70% confluency in DMEM (10% FBS, 1% Pen/Strep). Twenty-four hours following seeding, transient transfections were performed using Lipofectamine 2000 (Cat #: 11668019, Invitrogen, Carlsbad, CA, USA) according to the manufacturer's protocol without including additional transformation carrier DNA.

Ligand-induced BRET assays:

Twenty-four hours following transfection, HEK293T cells were washed with PBS and resuspended in FluoroBrite phenol red-free complete media (Cat #: A1896701, Life Technologies, Carlsbad, CA, USA) containing 5% FBS and 2 mM of L-glutamine (Cat #: 25030081, Life Technologies, Carlsbad, CA, USA). 100,000 cells/well were plated into poly-D-Lysine-coated (Cat #: P6403, Sigma–Aldrich, St. Louis, MO, USA) 96-well white polystyrene LumiNunc plates (Cat #: 10072151, Thermo Fisher Scientific, Waltham, MA, USA). After 24 hrs, the media was replaced with PBS (Cat #: 10010056, Gibco, Carlsbad, CA, USA) containing 10 mM of coelenterazine-h (Cat #: S2011, Promega, Madison, WI, USA) or 1:500 dilution of NanoGlo (Cat #: N1110, Promega, Madison, WI, USA). BRET measurements were taken every 30 sec – 2 min using a PHERAstar FS multi-mode microplate reader. Baseline measurements were taken after an initial 5 min incubation with coelenterazine-h or NanoGlo-containing PBS after which cells were then treated with either vehicle (PBS) or respective ligands. The resulting ligand-specific ratiometric BRET signals were normalized to vehicle producing the “ligand-induced BRET ratio”[21], followed by an additional normalization step to well-specific baseline readings. Ligand-induced measurements on the temporal scale is represented as the subsequent measurement after time point zero. Positive or negative incremental area under the curves (+iAUC/-iAUC) were calculated where noted. Each experiment was independently performed at least three times, each with at least three technical replicates for each group.

Receptor signaling and trafficking BRET Assays

Untagged hGLP-1R was purchased from Sino Biological Inc. (Cat #: HG13944-UT, Beijing, China), hGLP-1R-GFP was a kind gift from David Hodson (University of Birmingham, Birmingham, UK), and hGLP-1R-Rluc8 was a kind gift from Patrick Sexton (Monash University, Melbourne, Australia). Ga_s recruitment to the GLP-1R-GFP was quantified using mini-Ga_s, a protein probe that translocates to ligand-bound Ga_s-coupled GPCRs[22]. NES-Nluc-MiniGa_s was a gift from Kevin Pfleger (Harry Perkins Institute of Medical Research, Nedlands, WA, Australia). Intracellular cAMP was measured using the YFP-Epac-Rluc CAMYEL sensor[23]. hGLP-1R-RLUC8 internalization was quantified using the intracellular plasma membrane marker Venus-KRAS[24]. Venus-KRAS was a kind gift from Kevin Pfleger. GLP-1R-Rluc8 lysosomal co-localization was measured using Lamp1-mNeonGreen. Lamp1-mNeonGreen was a gift from Dorus Gadella (Addgene

plasmid # 98882). Time-dependent RXR/PPARg heterodimerization was measured using RXR-Rluc8 and PPARg2-YFP, both of which were kind gifts from Professor Vincent Ollendorf[25].

Gene expression analysis

For assessment of acute drug effects, animals were treated with the respective compounds 4 hrs prior to tissue harvesting. Dissected tissues were frozen immediately on dry ice, and RNA was isolated using RNeasy Mini Kits (Qiagen). mRNA levels were determined using TaqMan probes in custom-made low density array cards (ThermoFisher) or in single assays on a QuantStudio 7 Real-Time PCR system. Target gene expression was normalized to HPRT and fold change was calculated relative to vehicle treated controls.

Proteomics sample preparation

Frozen tissue samples were homogenized in 0.1 M Tris-HCl, pH 7.6, and 2% SDC, heated for 5 min at 95°C and sonicated (Diagenode Bioruptor at high intensity, 15 x 30s). 50 µg of protein was reduced and alkylated with 10 mM TCEP,40 mM CAA for 5 min at 40°C in the dark. Samples were digested with trypsin and LysC 1:50 (enzyme:protein) overnight at 37°C. Digested peptides were acidified to a final concentration of 1% TFA and loaded onto activated triple layer styrenedivinylbenzene–reversed phase sulfonated (SDB-RPS; 3 M Empore) STAGE tips. STAGE tips were washed with 100 µl ethylacetate 1% TFA, 100 µl 30% Methanol 1% TFA and 150 µl 0.2% TFA. Peptides were eluted with 60 µl SDB-RPS elution buffer (80% ACN, 5% NH4OH), concentrated in a SpeedVac for 40 min at 45°C, and dissolved in 10 µl MS loading buffer (2% ACN, 0.1% TFA).

LC-MS/MS analysis

Single-shot measurements were performed with 500 ng of purified peptides, determined by absorbance at 280 nm on a NanoDrop 2000. Peptides were loaded onto a 50-cm column, packed in-house with 1.9 µm C18 ReproSil particles (Dr. Maisch GmbH) with an EASY-nLC 1200 system (Thermo Fisher Scientific). Column temperature was kept at 60°C using a column oven. Peptides were eluted over 60 min using a binary buffer system consisting of buffer A (0.1% formic acid) and buffer B (80% ACN, 0.1% formic acid). In brief, the gradient started with 5% buffer B and increased stepwise to 45% over 45min, followed by a wash-out at 95% buffer B, all at a flowrate of 300 nl/min. Peptides were then transferred to the gas phase using electrospray ionization (ESI), pre-filtered by a FAIMS device (CV -50 V) before entering the Orbitrap Exploris 480 (Thermo Fisher Scientific) mass spectrometer. A data-independent (DIA) acquisition method was used, in which one full scan (300-1650 m/z, max. ion fill time of 45ms, normalized AGC target = 300%, R= 120.000 at 200 m/z) was followed by 66 tMS2 fragment scans of unequally-spaced windows

with 1 Th overlap, covering the same m/z range (fill time = 22 ms, normalized AGC target = 1000%, normalized HCD collision energy = 30%, R= 15.000).

Bioinformatic workflow and proteomic data analysis

DIA raw files were processed using Spectronaut version 14.5.200813.47784[26] using the directDIA function with default settings. Raw files from samples of the same tissue were processed together and searched against the mouse UniProt FASTA database (September 2014, 51,210 entries) and the provided MaxQuant contaminants list (245 entries). Spectronaut report files were then loaded into Perseus (v.1.6.2.3). In brief, quantified proteins were filtered for ≥ 3 valid values in at least one biological condition and annotations mapped from UniProtKB, Gene Ontology (GO), and the Kyoto Encyclopedia of Genes and Genomes (KEGG). Significantly up- or downregulated proteins between the conditions were determined by ANOVA (FDR 0.025).

Statistics

Statistical analyses were performed using the statistical tools implemented in GraphPad Prism8 (version 8.3.0). All data are shown as mean ± SEM. Differences between groups were assessed by 1-way ANOVA or 2-way ANOVA with time and treatment as co-variants followed by Bonferroni's post-hoc multiple comparison testing as indicated in the figure legends. A p-value < 0.05 was considered statistically significant.

Results

GLP-1/ Tesaglitazar shows GLP-1R-dependent PPARγ/RXR heterodimerization with preserved ability for GLP-1R activation, internalization and degradation

The GLP-1/Tesaglitazar conjugate was assembled on a validated GLP-1 analog backbone[27]. This analog (GLP-1-CEX) features the C-terminal extension derived from exendin-4, which was sequentially added to the human GLP-1 sequence that includes two substitutions (aminoisobutyric acid [Aib] at position 2 and glutamic acid (Glu) at position 16). Tesaglitazar was covalently attached to the side chain amine of the C-terminal lysine residue on the GLP-1-CEX backbone (henceforth just named GLP-1) via a gamma glutamic acid spacer (Figure 1a). In HEK293 cells transfected with a cDNA encoding human GLP-1R, GLP-1/Tesaglitazar showed comparable efficacy relative to GLP-1 in GLP-1R-mediated $G\alpha_s$ recruitment (Figure 1b,c) and cAMP production (Figure 1d). No difference was observed between GLP-1 and GLP-1/Tesaglitazar in ligand-induced GLP-1R internalization (Figure 1e,f) and lysosomal GLP-1R appearance, as indicated by comparable GLP-1R-Lamp1 co-localization following treatment with GLP-1 or GLP-1/Tesaglitazar (Figure 1g,h). Tesaglitazar alone had no effect on either GLP-1R Gαs recruitment, cAMP

production, GLP-1R internalization or GLP-1R-Lamp1 co-localization (Figure 1b-h). Consistent with the kinetic of ligand-induced GLP-1R internalization (Figure 1e), GLP-1/Tesaglitazar showed a delayed onset of PPARγ/RXR heterodimerization with comparable potency relative to Tesaglitazar after 30 min when tested in GLP-1R expressing HEK293 cells (Figure 1i,j). No meaningful PPARγ/RXR heterodimerization was observed by GLP-1/Tesaglitazar treatment in HEK293 cells that lack GLP-1R (Figure 1k,l). Thus, GLP-1/Tesaglitazar induces PPARγ/RXR heterodimerization in a GLP-1R-dependent manner and shows equal, yet not superior, efficacy as GLP-1 in activation, internalization, and degradation of GLP-1R.

GLP-1/ Tesaglitazar improves body weight, food intake, and glucose metabolism in DIO mice

In DIO mice, 14-day treatment with GLP-1/Tesaglitazar (50 nmol/kg/day) decreased body weight and food intake with superior potency relative to treatment with equimolar doses of GLP-1 or Tesaglitazar (Figure 2a,b). The decreased body weight in GLP-1/Tesaglitazar-treated mice was associated with a decrease in body fat mass, with only a slight but significant decrease in lean tissue mass (Figure 2c,d). GLP-1/Tesaglitazar, but not GLP-1 or Tesaglitazar alone, decreased levels of fasted blood glucose (Figure 2e). This was paralleled by a more significant decrease in levels of fasted insulin (Figure 2f), and improved insulin sensitivity relative to vehicle treated controls, as indicated by HOMA-IR (Figure 2g) and by direct assessment of insulin tolerance (Figure 2h,i). In isolated murine islets, GLP-1/Tesaglitazar showed preserved but slightly decreased ability to stimulate insulin secretion under conditions of high glucose relative to GLP-1 (Figure 2j). These data align with the demonstration that GLP-1/Tesaglitazar is not superior to GLP-1 in either GLP-1R activation, internalization or degradation (Figure 1b-h), and suggest that factors other than enhanced GLP-1R action in the β-cells contribute to the superior glucometabolic effect of GLP-1/Tesaglitazar. In line with our data showing that GLP-1/Tesaglitazar only induces PPAR/RXR heterodimerization in the presence of GLP-1R (Figure 1i-l), Tesaglitazar, but not GLP-1/Tesaglitazar, induced expression of known PPAR target genes in tissues that lack GLP-1R expression, notably the liver (*Fabp4* and *Plin2*) and skeletal muscle (*Arntl* and *Sema3c*) (Figure 2k-n). Daily treatment of DIO mice with GLP-1/Tesaglitazar at doses of 10, 25 or 50 nmol/kg/day showed no difference in plasma creatinine levels, relative to vehicle controls after 14-days of treatment, suggesting normal kidney function (Figure 2o).

GLP-1/Tesaglitazar also decreased body weight in lean mice with superior efficacy relative to equimolar treatment with either Tesaglitazar or to co-therapy of GLP-1 and Tesaglitazar (Figure 2p). Consistent with the observation that Tesaglitazar, but not GLP-1/Tesaglitazar, increased expression of PPAR target genes in the livers of mice that lack GLP-1R expression (Figure 2k-n), only treatment with Tesaglitazar, but not (equimolar doses of) GLP-1 or GLP-1/Tesaglitazar, reduced plasma cholesterol levels (Figure 2q). These data hence indicate that binding Tesaglitazar to the GLP-1 backbone prevents hepatic PPAR activation by Tesaglitazar. In line with the greater decrease in body weight and body fat mass in mice treated with GLP-1/Tesaglitazar (Figure 2a and c), plasma levels of triglycerides were decreased by treatment with GLP-1/Tesaglitazar but not with GLP-1 or Tesaglitazar alone (Figure 2r). No differences were observed in any of the treatment groups in markers indicative of liver damage (AST and ALT) (Figure 2s,t) or heart weight (Figure 2u). Collectively, these data show that GLP-1/Tesaglitazar is superior to the GLP-1 and

Tesaglitazar monotherapies in reducing body weight and food intake, and to improve glycemic control, and this is not accompanied by chances in markers indicative of liver function, (ALT, AST), kidney function (creatinine) or heart hypertrophy.

Single low-dose treatment with GLP-1/Tesaglitazar acutely improves glucose tolerance in DIO mice

Based on the insulin-sensitizing effect of GLP-1/Tesaglitazar in DIO mice (Figure 2h,i), we next assessed whether the acute glycemic benefits prevail even at doses subthreshold for GLP-1 to improve glucose metabolism. Bolus peripheral treatment of DIO mice with Tesaglitazar at doses of 10 and 100 nmol/kg acutely worsened intraperitoneal glucose tolerance (Figure 3a,b). When given at a dose of 100 nmol/kg, GLP-1 and GLP-1/Tesaglitazar both improved glucose tolerance with only slightly enhanced efficacy of the conjugate relative to GLP-1 (Figure 3c,d), which is not surprising as these doses far exceed the maximally efficacious doses of these GLP-1-based compounds. At a dose of 10 nmol/kg GLP-1/Tesaglitazar showed superior efficacy to improve glucose tolerance (Figure 3e,f) relative to GLP-1. Strikingly, at a dose of 3 nmol/kg, GLP-1 failed to improve glucose tolerance while the beneficial glycemic effect of GLP-1/Tesaglitazar fully prevailed (Figure 3g,h). These data indicate that GLP-1/Tesaglitazar possesses at low concentrations a substantially enhanced potency to acutely improve glucose tolerance relative to the GLP-1 monotherapy.

Low-dose GLP-1/Tesaglitazar chronically improves body weight and glucose handling in DIO mice

We next assessed whether daily low-dose chronic treatment with GLP-1/Tesaglitazar also affects energy and glucose tolerance in DIO mice. When given at a daily dose of 5 nmol/kg, 7-day treatment with GLP-1/Tesaglitazar decreased body weight and food intake in DIO mice, while mice treated with GLP-1 showed no difference in either body weight or food intake relative to vehicle controls (Figure 4a,b). Consistent with the lower body weight, GLP-1/Tesaglitazar decreased body fat mass relative to GLP-1 and to vehicle-treated mice (Figure 4c) with only a slight but significant decrease in lean tissue mass (Figure 4d). GLP-1/Tesaglitazar but not GLP-1 decreased levels of fasted blood glucose (Figure 4e), and GLP-1/Tesaglitazar further improved glucose tolerance relative to treatment with GLP-1 (Figure 4f,g).

The metabolic effects of GLP-1/Tesaglitazar depend on functional GLP-1R and are preserved in diabetic db/db mice

When given at a daily dose of 50 nmol/kg, 6-day treatment with GLP-1/Tesaglitazar robustly improved body weight, fat mass, food intake, blood glucose and glucose tolerance in DIO wildtype mice (Figure 5a-f), but not in DIO mice lacking the GLP-1 receptor (Figure 5g-l). These data indicate that the metabolic effects of GLP-1/Tesaglitazar require functional GLP-1R signaling. We next assessed whether the metabolic and glycemic benefits of GLP-1/Tesaglitazar translate from the HFD model to db/db mice with genetically induced diabetes and obesity. Consistent with the superior ability of GLP-1/Tesaglitazar to decrease body weight and to improve glucose metabolism in DIO mice (Figure 2a,e-i), GLP-1/Tesaglitazar (50 nmol/kg/day), but not equimolar treatment with GLP-1 or Tesaglitazar alone, decreased body weight in obese and diabetic db/db mice (Figure 6a). Consistent with the greater decrease in body weight, GLP-

1/Tesaglitazar significantly reduced food intake relative to treatment with GLP-1 or Tesaglitazar alone (Figure 6b) and this was paralleled by a greater decrease in fasted blood glucose (Figure 6c,d) and further improvement of insulin sensitivity (Figure 6e,f). Collectively, these data show that GLP-1/Tesaglitazar outperforms GLP-1 and Tesaglitazar to decrease body weight and improve glucose metabolism in mice with genetically-induced obesity and glucose intolerance. The observation that the metabolic effects of GLP-1/Tesaglitazar depend on functional GLP-1R *in vivo* align with our *in vitro* demonstration that GLP-1/Tesaglitazar fails to induce PPARγ/RXR heterodimerization in the absence of GLP-1R (Figure 1i-l).

LC/MS-based proteomics reveals novel PPAR-regulated targets engaged by GLP-1/Tesaglitazar in the hypothalamus

Based on recent data indicating that PPARγ might affect systemic energy metabolism via hypothalamic neurocircuitries[5,6], and since the glycemic benefits of GLP-1/Tesaglitazar are most pronounced after acute treatment (Figure 3g,h), we next assessed the response of the hypothalamic proteome of DIO mice after single peripheral drug treatment using LC/MS. In single-shot 60 min DIA analyses, we quantified more than 6,500 hypothalamic proteins (Figure 7a). High reproducibility was indicated by a median coefficient of variation (CV) <2% for all conditions. The abundance ranked plot of the entire measured proteome spans a dynamic range of six orders of magnitude of estimated absolute abundance covering neuronal marker proteins among various abundance levels (Supplementary Figure 1). Principal component analysis (PCA) revealed a clear separation of the treatment groups in the first component. GLP-1/Tesaglitazar induced a stronger PCA shift than GLP-1 or Tesaglitazar alone (Figure 7b). Choosing a stringent cut-off (ANOVA, FDR<0.025), 1,167 proteins exhibited statistically significant changes in their levels compared to vehicle-treated controls, thereby reflecting a strong proteomic response. Relative to vehicle-treated controls, we observed a solid pattern of GLP-1 responsive proteins in the hypothalamus, with 487 proteins being upregulated (Cluster 2) and 576 being downregulated by GLP-1 treatment (Cluster 3) (Figure 7c). Similar GLP-1 responsive protein patterns were observed after treatment with GLP-1/Tesaglitazar (Figure 7c,d). Enriched pathways (Fisher exact test, FDR<0.05) upregulated by GLP-1 and GLP-1/Tesaglitazar included signaling mechanisms implicated in neuronal projection, and regulation of transcription and endocytosis while pathways of TLR, mTOR, VEGF and MAPK signaling were downregulated (Figure 7e). Notably, we also found a unique and similar pattern of hypothalamic proteins that were acutely upregulated by Tesaglitazar and by GLP-1/Tesaglitazar, but not by treatment with GLP-1 (104 proteins were upregulated by treatment with Tesaglitazar and by GLP-1/Tesaglitazar, Cluster 1) (Figure 7c). Enriched pathways upregulated by Tesaglitazar and GLP-1/Tesaglitazar include mechanisms implicated in vesicle-mediated transport, neuron projection, Ca^{2+} signaling, (phospho)lipid biosynthesis and neurotransmitter transport (Figure 7e). Interestingly, GLP-1 and GLP-1/Tesaglitazar treatments affected the levels of several key kinases mediating metabolic signaling pathways (e.g. insulin signaling) (Figure 7f). Overall, the GLP-1/Tesaglitazar proteomic signature reflected a combination of the specific GLP-1 and Tesaglitazar responses, integrating the effects on metabolic pathways and neuronal functions of the individual components. Notably, we observed slightly decreased GLP-1-selective changes in the hypothalamic proteome by treatment with GLP-1/Tesaglitazar relative to GLP-1 (Figure 7c), which aligns

with our data in isolated islets showing somewhat decreased insulinotropic action of GLP-1/Tesaglitazar relative to GLP-1 (Fig. 2j). However, we observed stronger Tesaglitazar-selective changes in the proteome by treatment with GLP-1/Tesaglitazar relative to Tesaglitazar alone (Figure 7c). These data confirm that GLP-1/Tesaglitazar engages PPAR targets in the hypothalamus and suggest that the known high expression of GLP-1R in the hypothalamus allows for a favorable delivery of GLP-1/Tesaglitazar into this tissue. The enriched amplitude of PPAR-induced signaling observed with the GLP-1/Tesaglitazar conjugate is potentially due to selective biodistribution of the Tesaglitazar to GLP-1R positive tissues, as opposed to systemic biodistribution achieved with unconjugated Tesaglitazar treatment that would otherwise dilute the signaling amplitude.

Discussion

We here report the development and molecular characterization of a GLP-1 peptide biochemically modified for GLP-1R-dependent delivery of the PPARα/γ dual-agonist Tesaglitazar. We demonstrate that GLP-1/Tesaglitazar is comparably efficacious as GLP-1 to promote GLP-1R-mediated $G\alpha_s$ recruitment, cAMP production, as well as internalization and degradation of the GLP-1 receptor *in vitro*, but is superior in decreasing body weight and improving glucose metabolism *in vivo*. Consistent with the *in vitro* data showing that GLP-1/Tesaglitazar is not simply a GLP-1 analog of enhanced potency, we see comparable, yet not superior, stimulation of insulin secretion by GLP-1/Tesaglitazar in isolated murine islets relative to GLP-1. Rather, GLP-1/Tesaglitazar demonstrates unique pharmacodynamic properties by inducing PPARγ-RXR heterodimerization only in the presence of GLP-1R. This indicates that GLP-1/GLP1R interaction acts as a viable vector for Tesaglitazar intracellular delivery. This results in comparable efficacy relative to Tesaglitazar, yet with a notable delayed onset. This delayed onset of PPARγ-RXR heterodimerization by GLP-1/Tesaglitazar relative to Tesaglitazar is consistent with the observed time-dependent kinetics of ligand-induced GLP-1R internalization, and suggests that the rate of GLP-1R-mediated internalization of GLP-1/Tesaglitazar is critical to allow for an adequate induction of PPARγ-RXR heterodimerization and hence to promote PPAR target effects. Consistent with this, we show lack of GLP-1/Tesaglitazar effects in the GLP-1R negative tissues *in vivo*, notably liver and skeletal muscle, as well as in GLP-1R ko mice.

Consistent with a differential pharmacodynamic signature, treatment with GLP-1/Tesaglitazar led to greater reduction in body weight and food intake in DIO and db/db mice compared to treatment with GLP-1 or Tesaglitazar, whereas the glucoregulatory and weight loss actions were eliminated in GLP-1R deficient mice. Interestingly, GLP-1/Tesaglitazar was exceptionally potent to acutely improve glucose tolerance, particularly at very low doses subthreshold for either GLP-1 or Tesaglitazar alone. Our data in isolated islets suggest that this enhanced effectiveness is not mediated by enhanced insulin secretion. Although this will require further testing, it is possible that the enhanced glycemic effects of the conjugate may be mediated by glucoregulatory organs that receive feedback from the CNS, and specifically the hypothalamus. The aforementioned possibility would be in accordance with the differential hypothalamic proteomic signatures observed with GLP-1/Tesaglitazar relative to GLP-1 alone. By using LC/MS

proteomic analysis, we identified the hypothalamus as a target of GLP-1/Tesaglitazar, consistent with the known distribution pattern of the GLP-1 receptor in mice. This is consistent with the observation that the hypothalamus and the hindbrain are primary targets of fluorescently-labeled GLP-1R agonists[28,29] and aligns with the demonstration of high GLP-1R abundance in these brain regions[30,31]. PPARγ is expressed in various nuclei of the hypothalamus but not in the nucleus tractus solitarius (NTS) of the brainstem[5] and targeted overexpression of PPARγ in the hypothalamus decreases food intake in lean and DIO mice[6]. While the mechanistic underpinnings underlying food intake regulation by PPARγ remain largely unknown, in a hypothalamic cell line, stimulation of POMC expression by bisphenol A (BPA) is blocked by pretreatment with the PPARγ antagonist T0070907[32]. In summary, there is accumulating evidence indicating that PPARγ signaling engages hypothalamic neurocircuitries to control food intake, yet much more work is required to delineate precise mechanisms.

The proposed model of GLP-1-mediated delivery of a nuclear acting PPARα/γ dual-agonist aligns with previous manuscripts that have demonstrated the potential of this concept of peptide-mediated nuclear hormone delivery. In line with these notions, delivery of estrogen via GLP-1 improves body weight, glucose metabolism and dyslipidemia in DIO mice with greater efficacy relative to treatment with GLP-1 or estrogen alone and without detrimental estrogen effects in GLP-1R negative uterus or breast tissue[27]. The same GLP-1/estrogen conjugate outperformed GLP-1 and estrogen to restore β-cell mass and function in mice made diabetic by treatment with streptozotocin[33]. A molecule delivering dexamethasone via GLP-1 improved hypothalamic inflammation and astrogliosis with superior efficacy relative to GLP-1 or dexamethasone alone[34], while preferable delivery of thyroid hormone T3 via glucagon as the peptide carrier improved lipid and cholesterol metabolism with reduced off-target T3 effects in glucagon receptor negative tissues like the heart, skeletal muscle and the bone[35]. Also, the selective activation of PPARγ in NPY1R-expressing adipocytes using a molecule that covalently links Tesaglitazar to neuropeptide Y (NPY) was shown to enhance adipocyte differentiation and to prevent diabetes progression in db/db mice[36]. These provocative pharmacological findings reported with these peptide-mediated nuclear targeting set a foundation for further chemical refinement of the prototype chemical entities to improve their pharmaceutical properties. Further, this concept has provided a catalysis for targeting other effector molecules, including oligonucleotides for extra-hepatic modulation of specific gene targets[37,38].

Declarations

Acknowledgements

This work was funded by Novo Nordisk. MHT further received funding from the Alexander von Humboldt Foundation, the Helmholtz Alliance *ICEMED* & the Helmholtz Initiative on Personalized Medicine *iMed* by Helmholtz Association, the Helmholtz cross-program topic Metabolic Dysfunction and *the* European Research Council ERC AdG *HypoFlam* no. 695054. TDM received research funding from the German Research Foundation (DFG) TRR152 and TRR296 and the German Center for Diabetes Research (DZD e.V.). SMH received funding from the German Research Foundation (DFG) SFB1123. DJD is supported by

CIHR grant 154321, a Banting and Best Diabetes Centre Novo Nordisk Chair in Incretin biology and the Sinai Health Novo Nordisk Foundation Fund in regulatory peptides. CQ acknowledges support by INSERM, Agence Nationale de la Recherche (neuroIDobese, ANR-20-CE14-0046), Société Française d'Endocrinologie (Pfizer–SFE Prix de Recherche en Endocrinologie), Société Française de Nutrition and Société Francophone du Diabète. CGC received funding from the European research Council ERC STG [AstroNeuroCrosstalk no. 757393].

Author contributions

CQ, KS and AN, designed and performed experiments, analyzed and interpreted data and co-wrote the manuscript. BY, BF and RDdiM participated in drug development. FK, MB, AB-P, EB, GC, PC, GG, AH, NH, KK, EL, GM, DP-T and ZQ performed experiments and analyzed data. DJD provided research tools, discussed and interpreted data and critically revised the manuscript. CGC, SH, SH, HL, BS and NK participated in study design, supervision of experiments and interpretation of data. RDDiM, MHT, BF and TDM conceptualized the project, supervised experiments and analyzed and interpreted data. BF and TDM wrote the manuscript with support of CQ, KS and AN.

Declaration of Interests

MHT is a member of the scientific advisory board of ERX Pharmaceuticals, Cambridge, Mass. He was a member of the Research Cluster Advisory Panel (ReCAP) of the Novo Nordisk Foundation between 2017 and 2019. He attended a scientific advisory board meeting of the Novo Nordisk Foundation Center for Basic Metabolic Research, University of Copenhagen, in 2016. He received funding for his research projects by Novo Nordisk (2016–2020) and Sanofi-Aventis (2012–2019). He was a consultant for Bionorica SE (2013–2017), Menarini Ricerche S.p.A. (2016), and Bayer Pharma AG Berlin (2016). As former Director of the Helmholtz Diabetes Center and the Institute for Diabetes and Obesity at Helmholtz Zentrum München (2011–2018), and since 2018, as CEO of Helmholtz Zentrum München, he has been responsible for collaborations with a multitude of companies and institutions, worldwide. In this capacity, he discussed potential projects with and has signed/signs contracts for his institute(s) and for the staff for research funding and/or collaborations with industry and academia, worldwide, including but not limited to pharmaceutical corporations like Boehringer Ingelheim, Eli Lilly, Novo Nordisk, Medigene, Arbormed, BioSyngen, and others. In this role, he was/is further responsible for commercial technology transfer activities of his institute(s), including diabetes related patent portfolios of Helmholtz Zentrum München as, e.g., WO/2016/188932 A2 or WO/2017/194499 A1. MHT confirms that to the best of his knowledge none of the above funding sources were involved in the preparation of this paper. TDM and K.S. receive research funding by Novo Nordisk. DJD has received speaking and consulting fees from Eli

Lilly, Forkhead Biopharmaceuticals, KAllyope, Merck, Novo Nordisk Inc and Pfizer Inc. Mt. Sinai Hospital receives funding for preclinical studies in the Drucker lab from Novo Nordisk and Pfizer Inc. RDDiM is a co-inventor on intellectual property owned by Indiana University and licensed to Novo Nordisk. He was previously employed by Novo Nordisk. BF and BY are current employees of Novo Nordisk.

References

1. Fievet, C., Fruchart, J. C. & Staels, B. PPARalpha and PPARgamma dual agonists for the treatment of type 2 diabetes and the metabolic syndrome. *Curr Opin Pharmacol* **6**, 606–614, doi:10.1016/j.coph.2006.06.009 (2006).
2. Montaigne, D., Butruille, L. & Staels, B. PPAR control of metabolism and cardiovascular functions. *Nat Rev Cardiol*, doi:10.1038/s41569-021-00569-6 (2021).
3. Frick, M. H. *et al.* Helsinki Heart Study: primary-prevention trial with gemfibrozil in middle-aged men with dyslipidemia. Safety of treatment, changes in risk factors, and incidence of coronary heart disease. *N Engl J Med* **317**, 1237–1245, doi:10.1056/NEJM198711123172001 (1987).
4. Gross, B., Pawlak, M., Lefebvre, P. & Staels, B. PPARs in obesity-induced T2DM, dyslipidaemia and NAFLD. *Nat Rev Endocrinol* **13**, 36–49, doi:10.1038/nrendo.2016.135 (2017).
5. Sarruf, D. A. *et al.* Expression of peroxisome proliferator-activated receptor-gamma in key neuronal subsets regulating glucose metabolism and energy homeostasis. *Endocrinology* **150**, 707–712, doi:10.1210/en.2008-0899 (2009).
6. Li, Q. *et al.* Hypothalamic peroxisome proliferator-activated receptor gamma regulates ghrelin production and food intake. *Neuropeptides* **69**, 39–45, doi:10.1016/j.npep.2018.04.002 (2018).
7. Ryan, K. K. *et al.* A role for central nervous system PPAR-gamma in the regulation of energy balance. *Nat Med* **17**, 623–626, doi:10.1038/nm.2349 (2011).
8. Dubois, V., Eeckhoute, J., Lefebvre, P. & Staels, B. Distinct but complementary contributions of PPAR isotypes to energy homeostasis. *J Clin Invest* **127**, 1202–1214, doi:10.1172/JCI88894 (2017).
9. Lu, M. *et al.* Brain PPAR-gamma promotes obesity and is required for the insulin-sensitizing effect of thiazolidinediones. *Nat Med* **17**, 618–622, doi:10.1038/nm.2332 (2011).
10. Dormandy, J. A. *et al.* Secondary prevention of macrovascular events in patients with type 2 diabetes in the PROactive Study (PROspective pioglitAzone Clinical Trial In macroVascular Events): a randomised controlled trial. *Lancet* **366**, 1279–1289, doi:10.1016/S0140-6736(05)67528-9 (2005).
11. Jun, M. *et al.* Effects of fibrates on cardiovascular outcomes: a systematic review and meta-analysis. *Lancet* **375**, 1875–1884, doi:10.1016/S0140-6736(10)60656-3 (2010).
12. Kendall, D. M. *et al.* Improvement of glycemic control, triglycerides, and HDL cholesterol levels with muraglitazar, a dual (alpha/gamma) peroxisome proliferator-activated receptor activator, in patients with type 2 diabetes inadequately controlled with metformin monotherapy: A double-blind, randomized, pioglitazone-comparative study. *Diabetes Care* **29**, 1016–1023, doi:10.2337/diacare.2951016 (2006).

13. Ratner, R. E., Parikh, S., Tou, C. & Group, G. S. Efficacy, safety and tolerability of tesaglitazar when added to the therapeutic regimen of poorly controlled insulin-treated patients with type 2 diabetes. *Diab Vasc Dis Res* **4**, 214–221, doi:10.3132/dvdr.2007.042 (2007).
14. Balakumar, P., Mahadevan, N. & Sambathkumar, R. A Contemporary Overview of PPARalpha/gamma Dual Agonists for the Management of Diabetic Dyslipidemia. *Curr Mol Pharmacol* **12**, 195–201, doi:10.2174/1874467212666190111165015 (2019).
15. Rubenstrunk, A., Hanf, R., Hum, D. W., Fruchart, J. C. & Staels, B. Safety issues and prospects for future generations of PPAR modulators. *Biochim Biophys Acta* **1771**, 1065–1081, doi:10.1016/j.bbalip.2007.02.003 (2007).
16. Bays, H., McElhattan, J., Bryzinski, B. S. & Group, G. S. A double-blind, randomised trial of tesaglitazar versus pioglitazone in patients with type 2 diabetes mellitus. *Diab Vasc Dis Res* **4**, 181–193, doi:10.3132/dvdr.2007.039 (2007).
17. Goke, B., Gause-Nilsson, I., Persson, A. & Group, G. S. The effects of tesaglitazar as add-on treatment to metformin in patients with poorly controlled type 2 diabetes. *Diab Vasc Dis Res* **4**, 204–213, doi:10.3132/dvdr.2007.041 (2007).
18. Goldstein, B. J., Rosenstock, J., Anzalone, D., Tou, C. & Ohman, K. P. Effect of tesaglitazar, a dual PPAR alpha/gamma agonist, on glucose and lipid abnormalities in patients with type 2 diabetes: a 12-week dose-ranging trial. *Curr Med Res Opin* **22**, 2575–2590, doi:10.1185/030079906x154169 (2006).
19. Hamren, B., Ohman, K. P., Svensson, M. K. & Karlsson, M. O. Pharmacokinetic-pharmacodynamic assessment of the interrelationships between tesaglitazar exposure and renal function in patients with type 2 diabetes mellitus. *J Clin Pharmacol* **52**, 1317–1327, doi:10.1177/0091270011416937 (2012).
20. Wilding, J. P., Gause-Nilsson, I., Persson, A. & Group, G. S. Tesaglitazar, as add-on therapy to sulphonylurea, dose-dependently improves glucose and lipid abnormalities in patients with type 2 diabetes. *Diab Vasc Dis Res* **4**, 194–203, doi:10.3132/dvdr.2007.040 (2007).
21. Porrello, E. R. *et al.* Heteromerization of angiotensin receptors changes trafficking and arrestin recruitment profiles. *Cell Signal* **23**, 1767–1776, doi:10.1016/j.cellsig.2011.06.011 (2011).
22. Wan, Q. *et al.* Mini G protein probes for active G protein-coupled receptors (GPCRs) in live cells. *J Biol Chem* **293**, 7466–7473, doi:10.1074/jbc.RA118.001975 (2018).
23. Jiang, L. I. *et al.* Use of a cAMP BRET sensor to characterize a novel regulation of cAMP by the sphingosine 1-phosphate/G13 pathway. *J Biol Chem* **282**, 10576–10584, doi:10.1074/jbc.M609695200 (2007).
24. Lan, T. H., Kuravi, S. & Lambert, N. A. Internalization dissociates beta2-adrenergic receptors. *PLoS One* **6**, e17361, doi:10.1371/journal.pone.0017361 (2011).
25. Mulero, M., Perroy, J., Federici, C., Cabello, G. & Ollendorff, V. Analysis of RXR/THR and RXR/PPARG2 heterodimerization by bioluminescence resonance energy transfer (BRET). *PLoS One* **8**, e84569, doi:10.1371/journal.pone.0084569 (2013).

26. Bruderer, R. *et al.* Extending the limits of quantitative proteome profiling with data-independent acquisition and application to acetaminophen-treated three-dimensional liver microtissues. *Mol Cell Proteomics* **14**, 1400–1410, doi:10.1074/mcp.M114.044305 (2015).
27. Finan, B. *et al.* Targeted estrogen delivery reverses the metabolic syndrome. *Nat Med* **18**, 1847–1856, doi:10.1038/nm.3009 (2012).
28. Gabery, S. *et al.* Semaglutide lowers body weight in rodents via distributed neural pathways. *JCI Insight* **5**, doi:10.1172/jci.insight.133429 (2020).
29. Salinas, C. B. G. *et al.* Integrated Brain Atlas for Unbiased Mapping of Nervous System Effects Following Liraglutide Treatment. *Sci Rep* **8**, 10310, doi:10.1038/s41598-018-28496-6 (2018).
30. Heppner, K. M. *et al.* Expression and distribution of glucagon-like peptide-1 receptor mRNA, protein and binding in the male nonhuman primate (Macaca mulatta) brain. *Endocrinology* **156**, 255–267, doi:10.1210/en.2014-1675 (2015).
31. Jensen, C. B. *et al.* Characterization of the Glucagonlike Peptide-1 Receptor in Male Mouse Brain Using a Novel Antibody and In Situ Hybridization. *Endocrinology* **159**, 665–675, doi:10.1210/en.2017-00812 (2018).
32. Salehi, A., Loganathan, N. & Belsham, D. D. Bisphenol A induces Pomc gene expression through neuroinflammatory and PPARgamma nuclear receptor-mediated mechanisms in POMC-expressing hypothalamic neuronal models. *Mol Cell Endocrinol* **479**, 12–19, doi:10.1016/j.mce.2018.08.009 (2019).
33. Sachs, S. *et al.* Targeted pharmacological therapy restores beta-cell function for diabetes remission. *Nat Metab* **2**, 192–209, doi:10.1038/s42255-020-0171-3 (2020).
34. Quarta, C. *et al.* Molecular Integration of Incretin and Glucocorticoid Action Reverses Immunometabolic Dysfunction and Obesity. *Cell Metab* **26**, 620-632 e626, doi:10.1016/j.cmet.2017.08.023 (2017).
35. Finan, B. *et al.* Chemical Hybridization of Glucagon and Thyroid Hormone Optimizes Therapeutic Impact for Metabolic Disease. *Cell* **167**, 843-857 e814, doi:10.1016/j.cell.2016.09.014 (2016).
36. Wittrisch, S. *et al.* NPY1R-targeted peptide-mediated delivery of a dual PPARalpha/gamma agonist to adipocytes enhances adipogenesis and prevents diabetes progression. *Mol Metab* **31**, 163–180, doi:10.1016/j.molmet.2019.11.009 (2020).
37. Ammala, C. *et al.* Targeted delivery of antisense oligonucleotides to pancreatic beta-cells. *Sci Adv* **4**, eaat3386, doi:10.1126/sciadv.aat3386 (2018).
38. Nikan, M. *et al.* Targeted Delivery of Antisense Oligonucleotides Using Neurotensin Peptides. *J Med Chem* **63**, 8471–8484, doi:10.1021/acs.jmedchem.0c00840 (2020).

Figures

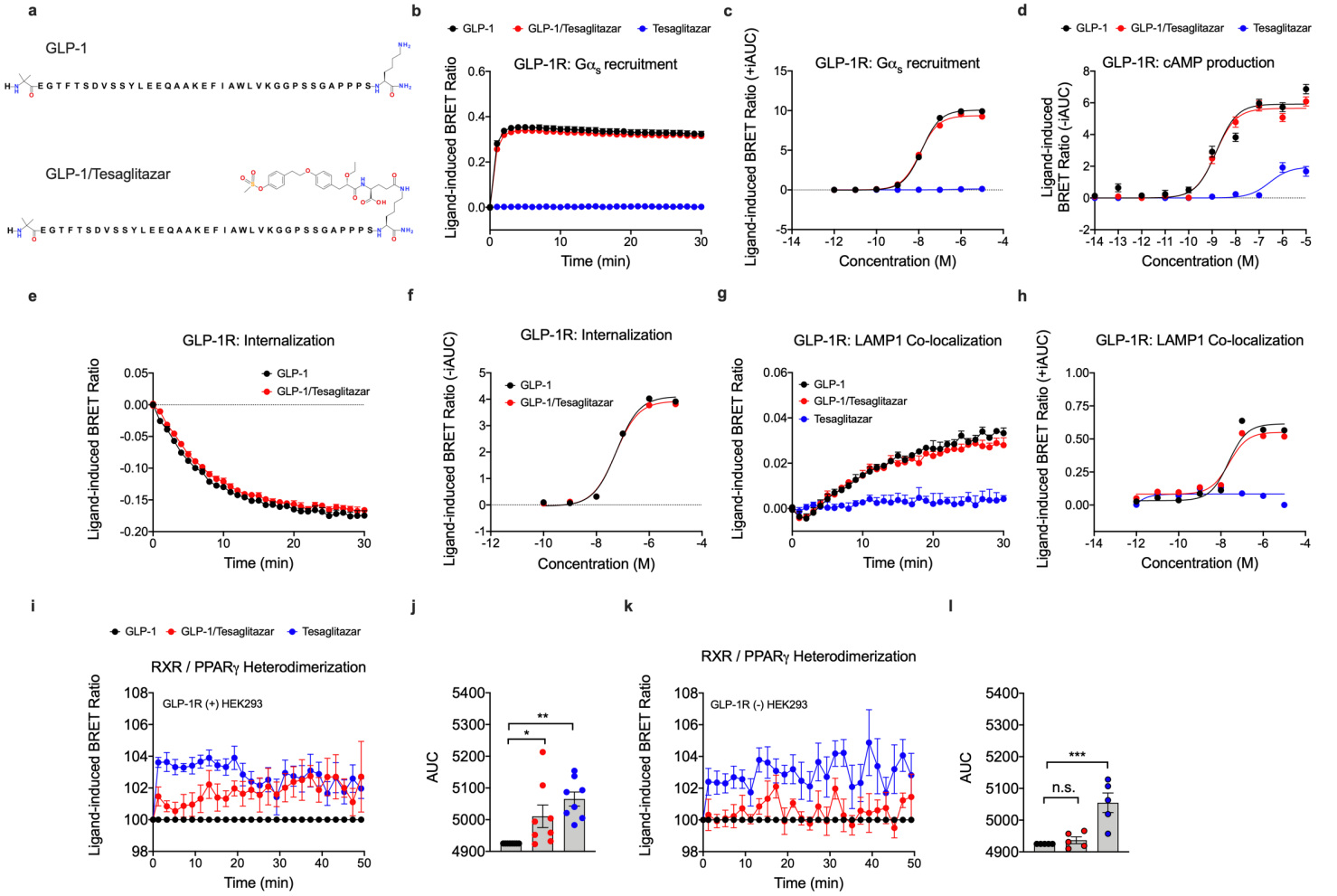

Figure 1

Effects of GLP-1/Tesaglitazar on GLP-1R signaling, trafficking, and nuclear hormone heterodimerization in HEK293 cells. Chemical structures of the GLP-1 analog (top) and GLP-1/Tesaglitazar conjugate (bottom) (a). Temporal resolution (1μM) (b) and dose-responses (c) for ligand-induced recruitment of Nluc-tagged Mini-Gαs to hGLP-1R-GFP. Dose-response curves of cAMP production in hGLP-1R+ HEK293T cells (d). Temporal resolution (1μM) (e) and dose-response curves (f) for ligand-induced hGLP-1R-Rluc8 internalization as measured by loss of BRET with plasma membrane marker Venus-KRAS. Temporal resolution (1μM) (g) and dose-response curves (h) for ligand-induced hGLP-1R-Rluc8 co-localization with the terminal lysosome marker Lamp1-mNeonGreen. Temporal resolution (i) and AUC (j) of ligand-induced (1μM) RXR-Rluc8 and PPARγ2-YFP heterodimerization in hGLP-1R(+) HEK293T cells and hGLP-1R(-) HEK293T cells (k, l). iAUC representation of vehicle and baseline-corrected 30 min (Gαs, cAMP, receptor internalization, lysosomal co-localization) or 50 min (RXR/PPARγ heterodimerization) temporal responses of each agonist. Three (a-h) or eight (i-l) independent experiments were performed with at least three technical replicates per group. Data were analyzed using one-way-ANOVA. Date represent mean ± SEM; asterisks indicate * p<0.05; ** p<0.01 and *** p<0.001.

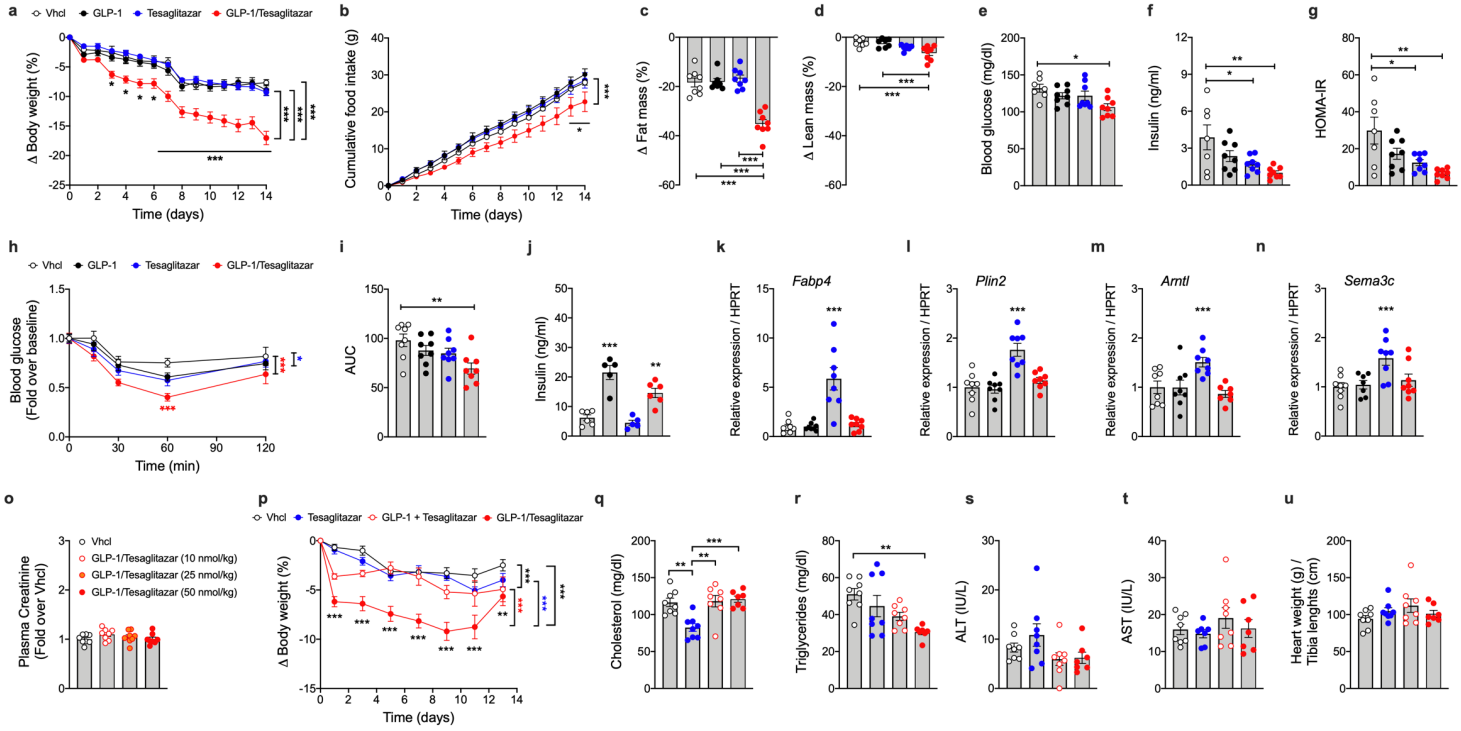

Figure 2

GLP-1/Tesaglitazar improves body weight and glucose metabolism in DIO mice and decreases body weight and lipid metabolism in lean mice. Effects on body weight (a), cumulative food intake (assessed per cage in double-house mice) (b) and change of fat and lean tissue mass (c,d) in 34-wk old male DIO mice treated for 14-days with 50 nmol/kg of either GLP-1, Tesaglitazar or GLP-1/Tesaglitazar (N=7-8 mice each group). Fasting levels of blood glucose (e) and insulin (f) as well as HOMA-IR at study day 7 (N=7-8 mice each group) (g). Intraperitoneal insulin tolerance (ipITT) assessed at day 14 (N=8 each group) (h, i). Glucose-stimulated insulin secretion in isolated murine islets harvested from N=3 14-wk old male wildtype C57BL/6J mice and treated with 3 nmol of the drugs under conditions of 16.8 mM glucose (N=5-6 independent wells per treatment) (j). Expression of Fabp4 and Plin2 in liver (k,l) and of Arntl and Sema3c in skeletal muscle (m,n) of 30-wk weak old male DIO mice treated for 3-days at a dose of 50 nmol/kg/day (N=7-8 mice each group). Plasma levels of creatinine in 44-wk old male DIO mice treated for 14-days with GLP-1/Tesaglitazar at a dose of either 10, 25 or 50 nmol/kg/day (N=8 mice each group) (o). Changes in body weight (p), plasma levels of cholesterol (q), triglycerides (r), aspartate-aminotransferase (s), alanine-transferase (t) as well as heart weight (u) in 16-wk old male lean mice after 14-days of treatment (50 nmol/kg/day). Data represent means ± SEM. Data in panel a, b, h and p have been analyzed by 2-way ANOVA with Bonferroni post-hoc comparison for individual time points. Data in panel c-g, i-n and q-u have been analyzed by 1-way ANOVA using the Bonferroni's multiple comparison test. Asterisks indicate * p<0.05, ** p<0.01, *** p<0.001.

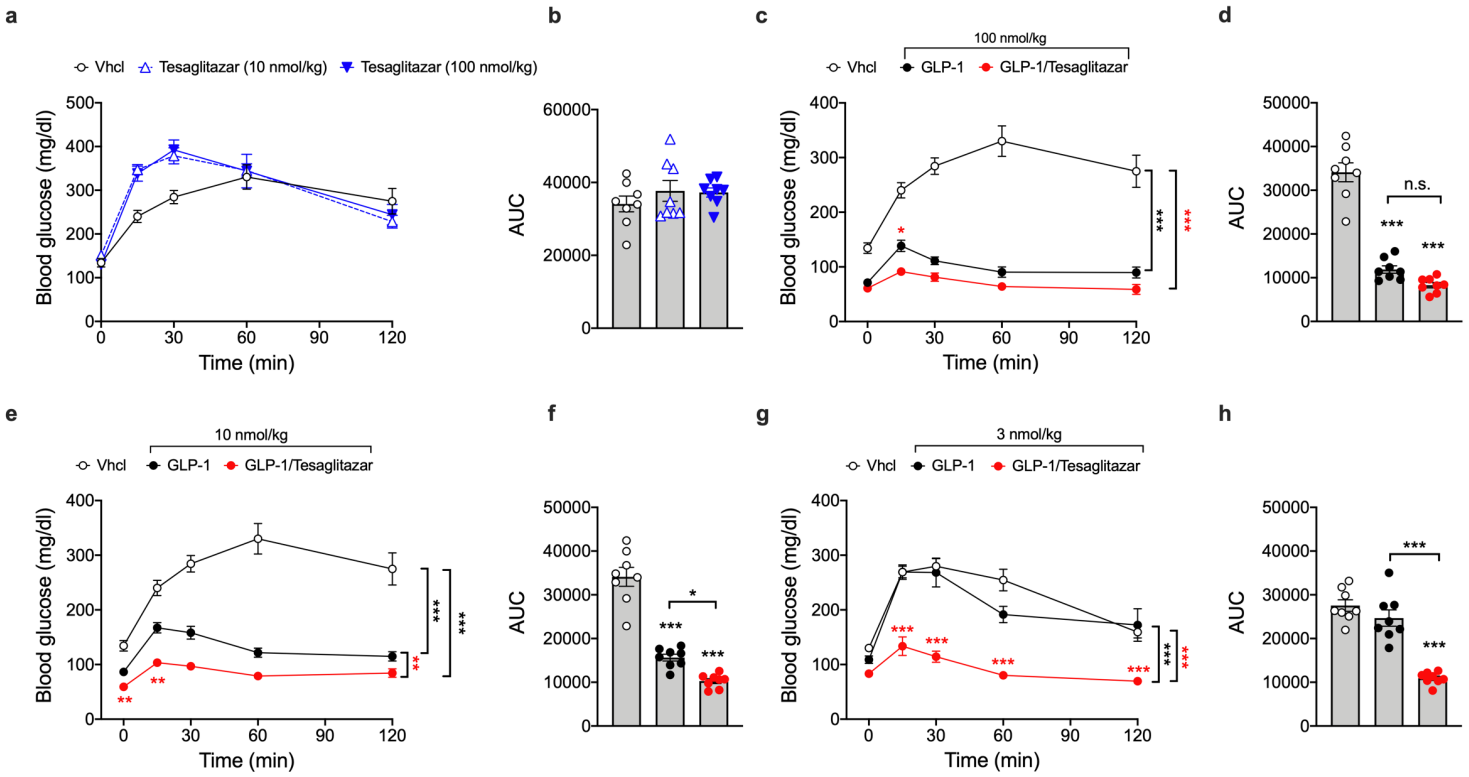

Figure 3

Acute glycemic benefits of GLP-1/Tesaglitazar prevail at low drug concentrations in DIO mice. Intraperitoneal glucose tolerance (ipGTT) in 34-wk old male DIO mice 6-hrs after treatment with Tesaglitazar at a dose of either 10 or 100 nmol/kg (a,b), or with GLP-1 or GLP-1/Tesaglitazar at a dose of either 100 nmol/kg (c,d), 10 nmol/kg (e,f), or 3 nmol/kg (g,h). N=8 mice each group. Data represent means ± SEM. Data in panel A, C, E and G have been analyzed by 2-way ANOVA with Bonferroni post-hoc comparison for individual time points. Data in panel b, d, f and h have been analyzed by 1-way ANOVA using Bonferroni's multiple comparison test. Asterisks indicate * p<0.05, ** p<0.01, *** p<0.001.

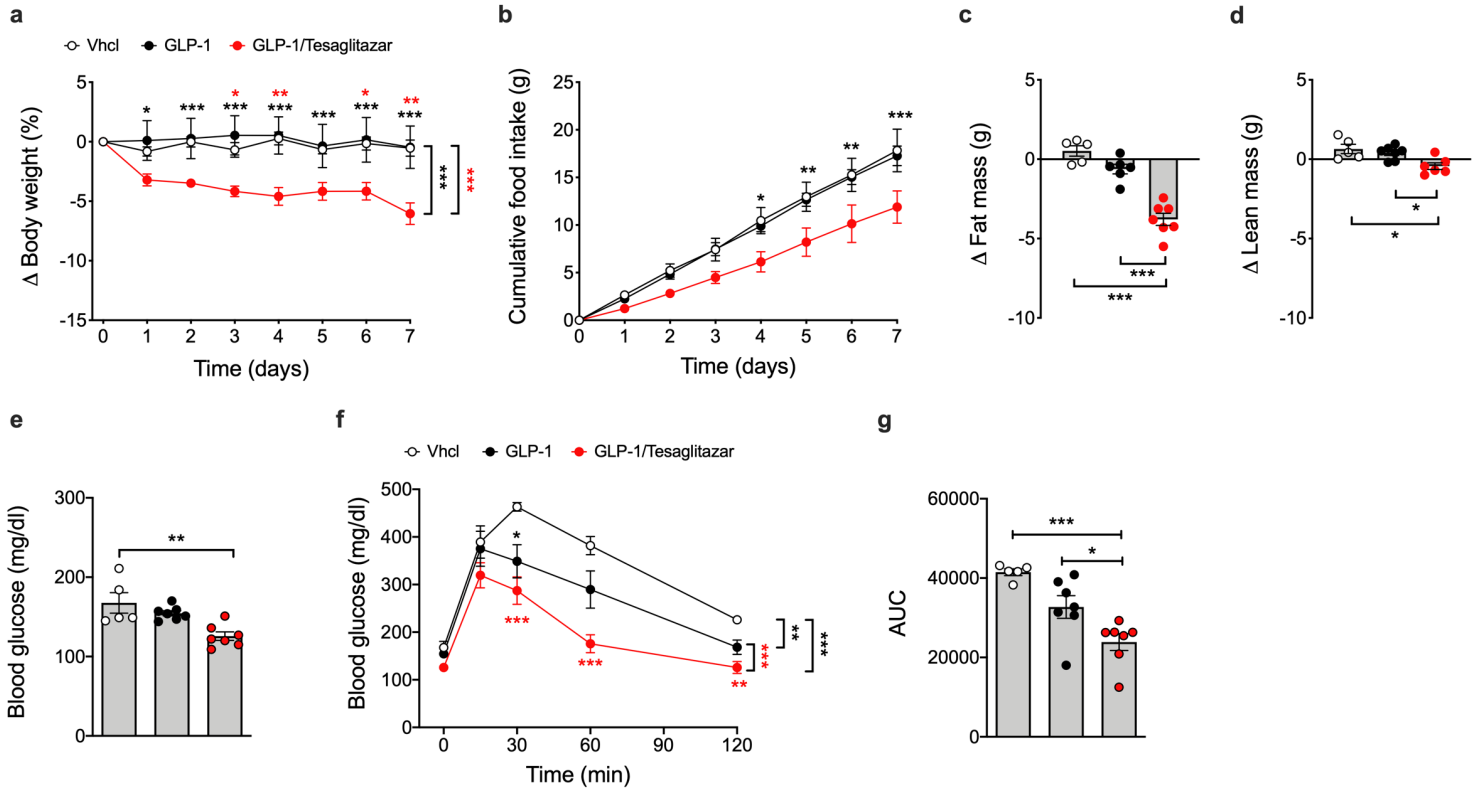

Figure 4

Chronic low-dose treatment with GLP-1/Tesaglitazar improves body weight and glucose metabolism in DIO mice. Body weight (a), cumulative food intake, assessed per cage in double-housed mice, (b) and change in fat and lean tissue mass (c,d) of 36-wk old DIO mice treated daily for 7 days with either vehicle or 5 nmol/kg/day of either GLP-1 or GLP-1/Tesaglitazar (N=5-7 mice each group). Fasting levels of blood glucose (e) and intraperitoneal glucose tolerance (ipGTT) in N=5-7 mice each group (f,g). Data in panel a, b, and f have been analyzed by 2-way ANOVA with Bonferroni post-hoc comparison for individual time points. Data in panel c, d, e and g have been analyzed by 1-way ANOVA using the Bonferroni's multiple comparison test. Data represent means ± SEM; asterisks indicate * p<0.05, ** p<0.01, *** p<0.001.

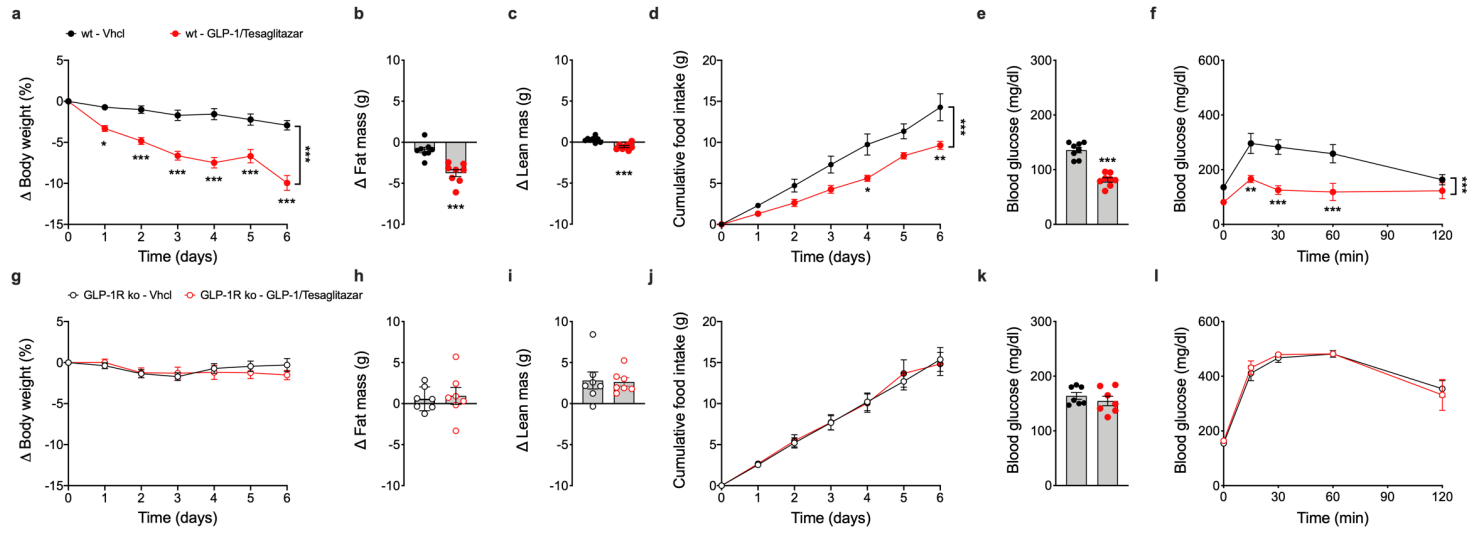

Figure 5

GLP-1/Tesaglitazar fails to affect body weight and glucose metabolism in obese GLP-1R ko mice. Body weight (a,g), change in fat and lean tissue mass (b,c, h,i), cumulative food intake (d,j), blood glucose (e,k) and intraperitoneal glucose tolerance (f,l) in 36-wk old male diet-induced obese wildtype (a-f) or GLP-1R ko mice (g-l) treated for 6-days with either Vehicle or 50 nmol/kg/day of GLP-1/Tesaglitazar. N=7-8 mice each group. Data in panel a, d, f, g, j, and l have been analyzed by 2-way ANOVA with Bonferroni post-hoc comparison for individual time points. Data in panel b, c, e, h, i and k have been analyzed by 1-way ANOVA using the Bonferroni's multiple comparison test. Data represent means ± SEM; asterisks indicate * p<0.05, ** p<0.01, *** p<0.001. Food intake (d,j) was assessed per cage in double-housed mice.

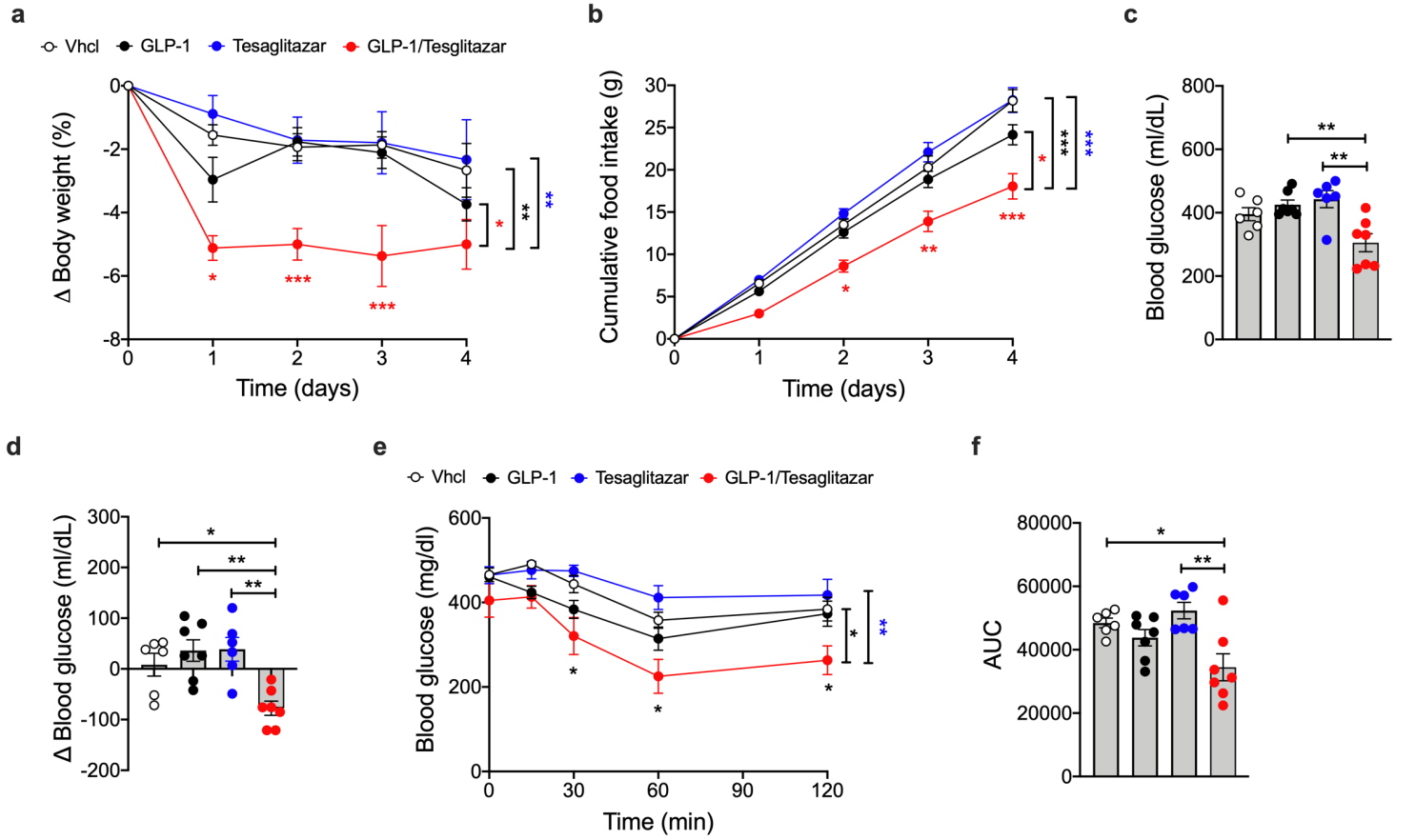

Figure 6

GLP-1/Tesaglitazar but not GLP-1 lowers body weight and improves glucose handling in obese db/db mice. Body weight (a), cumulative food intake (b), plasma glucose (c), change in blood glucose (d) and glucose tolerance (e,f) in 6 wk-old obese db/db mice treated for 4-days with either Vhcl or 50 nmol/kg/day or either GLP-1, Tesaglitazar or GLP-1/Tesaglitazar (N=6-7 mice each group). Data in panel a, b, and e have been analyzed by 2-way ANOVA with Bonferroni post-hoc comparison for individual time points. Data in panel c, d, and f have been analyzed by 1-way ANOVA using the Bonferroni's multiple comparison test. Data represent means ± SEM; asterisks indicate * p<0.05, ** p<0.01, *** p<0.001. Food intake (b) was assessed per cage in double-housed mice.

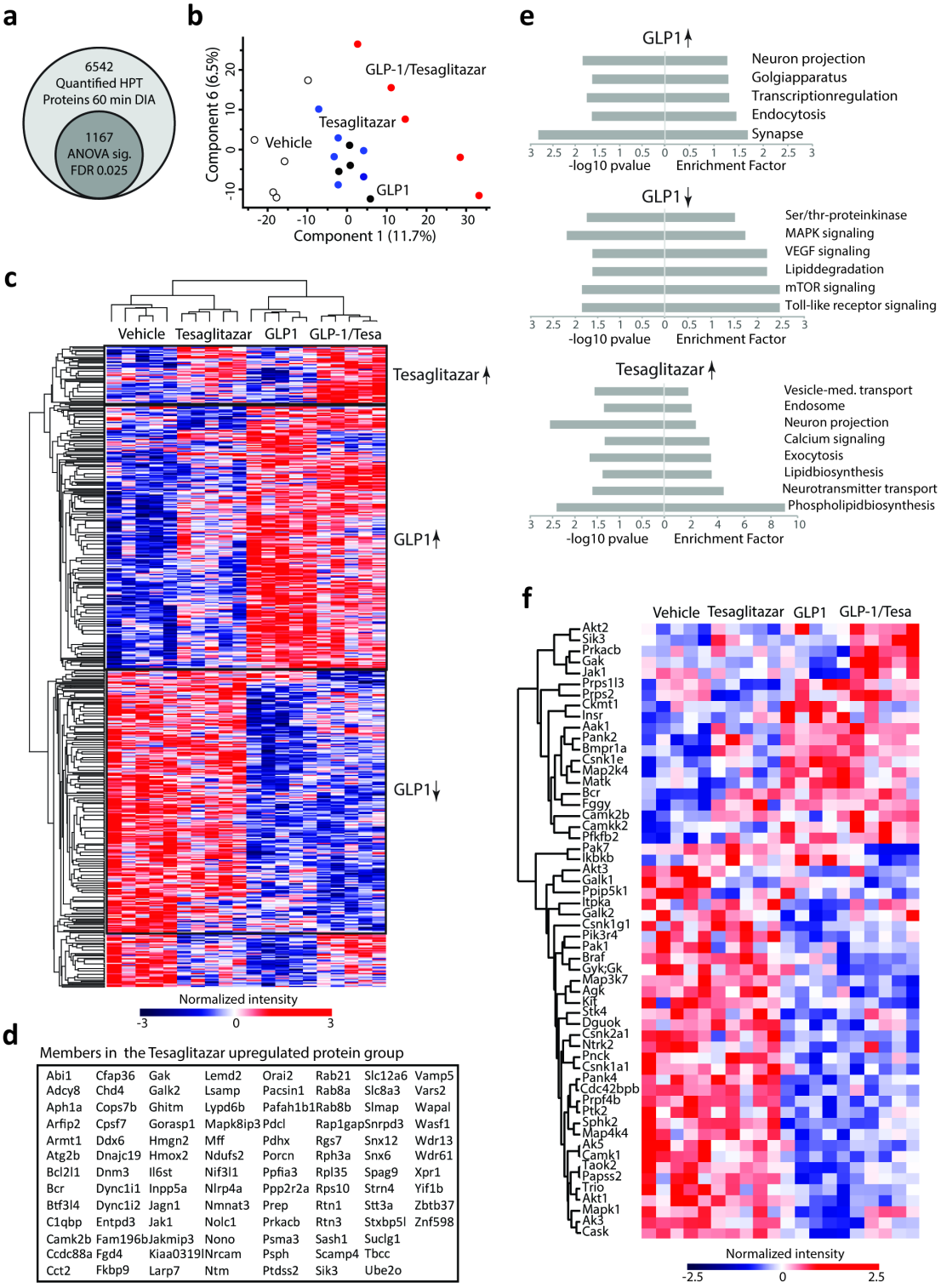

Figure 7

Proteomic changes in the hypothalamus of C57Bl/6J DIO mice after treatment with GLP-1, Tesaglitazar, or GLP-1/Tesaglitazar. Total number of quantified protein groups across all samples, as well as significantly changed number of proteins as determined by ANOVA (FDR<0.05) (a). Principal component analysis (PCA) of proteomic samples (b) and heat map of z-scored protein intensities among all significantly changed proteins (c). List of proteins upregulated by Tesaglitazar and by GLP-1/Tesaglitazar

(d). Selected gene annotations positively enriched in the specific treatment groups (e) and heat map of kinases significantly changed (ANOVA; FDR<0.05) by the respective treatment groups (f). Proteins are grouped by hierarchical clustering, coloring represents z-scored protein intensities.

Supplementary Files

This is a list of supplementary files associated with this preprint. Click to download.

- Suppl.Fig.1.tif